Behavior of Electron Wave Functions near the Atomic Nucleus and Normalization Screening Theory in the Atomic Photoeffect*

R. H. Pratt and H. K. Tseng
Department of Physics, University of Pittsburgh, Pittsburgh, Pennsylvania 15213
(Received 1 October 1971)

The behavior of electron wave functions near but outside the atomic nucleus is discussed. It is shown that point-Coulomb shapes persist to quite large distances ($r \cong 5\lambda\!\!\!^{-}_e$, where $\lambda\!\!\!^{-}_e$ is the Compton electronic wavelength) for bound states and also for energy-shifted continuum states. The screening effects on continuum-state normalizations cancel the screening effects on the kinematic factor pE in cross sections. These results are used to examine the normalization screening theory in atomic photoeffect, which is characterized by distances both small on an atomic scale and large compared to the size of the nucleus. It is argued that this theory, which describes screening effects simply as a change in normalization, can be good to 1% for photon energies more than 10 keV above the K-shell threshold in Al, 30 keV in Cu, 60 keV in Sn, 150 keV in Pb, and 200 keV in U. This agrees well in order of magnitude with exact numerical calculations.

I. INTRODUCTION

Near but outside the nucleus of an atom an electron sees a point-Coulomb potential corresponding to the nuclear charge Z. The electron wave function has a hydrogenlike shape; the only effect of atomic electrons, as described by a central potential $V(r)$ deviating from the point-Coulomb form, is to modify the normalization.[1(a)] This change in normalization is significant both for bound states and for low-energy continuum states.

This analysis of electron wave functions permits a simplified discussion of processes characterized by small distances on an atomic scale: Atomic-electron screening may be ignored except as an external multiplicative factor. One such process is orbital electron capture by a nucleus, since only the region of overlap between electron and nucleus contributes; Brysk and Rose[1(b)] summarized the argument and gave the K- and L-shell normalization changes due to screening as well as the further changes due to finite nuclear size. In ordinary β decay, on the contrary, the energy of the emitted continuum electrons is ordinarily large enough that screening effects are unimportant.[1(a)]

It is less obvious that the analysis applies to atomic photoelectric effect. Pratt[2] some time ago argued that over a wide energy range of photon energies electron-Compton-wavelength distances ($r = 1$) dominate the process and that at such distances the normalization screening theory that we have described still applies; applications were made in the MeV ranges and later extended below 100 keV by Schmickley and Pratt.[3] We will give and extend these arguments shortly. If they hold for photoeffect, it is not surprising that they also hold for internal conversion, where the real photon is replaced by a virtual photon from the nucleus—Band, Sliv, and Trzhaskovskaya[4] have recently demonstrated explicitly the dominance of electron-Compton-wavelength distances in internal conversion. For the photoeffect, a striking consequence of the analysis is that the shapes of the angular distributions of photoelectrons, and the polarization correlations as well, are independent of screening. Simple relations among cross sections from different shells also follow. Another consequence is that the "standard" screening theory (inner and outer screening, effective charge $Z_{\text{eff}} = Z - s$) is incorrect.[2] Similar results must follow in internal conversion. Recently, Tseng and Pratt[5] have verified that the only significant effect of atomic-electron screening on low-energy atomic-field pair production cross sections also comes from the change in normalizations of the continuum-positron-state and the continuum-electron-state wave functions; thus similar results may be obtained for the dependence of threshold pair production on screening. Photoeffect, internal conversion, and threshold pair production are examples of processes characterized by small distances on an atomic scale, but not small enough distances for nuclear size effects to enter. (Nuclear size effects require large momentum transfers, which even for high-energy photoeffect occurs only at large angles, making a negligible contribution to the total cross section.)

Recent numerical calculations of Ron and Scofield[6] suggest that the normalization screening theory of photoeffect works at lower energies than had been anticipated, in some cases as low as 10 keV. This has led us to examine the theory in greater detail. In Sec. II we estimate screening effects on electron wave functions, bound and continuum, and determine at what radius deviations from the point-Coulomb shape become important.

We compare our expectations with numerical calculations and indeed verify that point-Coulomb shapes persist to quite large distances ($r \cong 5$) for bound states, independent of the choice of screened potentials. For reference we tabulate the square of the ratio of the Hartree-Fock-Slater (HFS)[7] to point-Coulomb bound-state normalization constants. For continuum wave functions we find similar results, particularly when the comparison is made between Coulomb functions and screened functions of shifted energy appropriate to the K-shell photoeffect. In Sec. III we use this information to analyze the photoeffect. We estimate the dominant regions in r, and then estimate in what ranges (of Z, energy, shell) and with what accuracy photoelectric cross sections can be obtained from the normalization screening theory. We compare our predictions with numerical calculations.

II. BEHAVIOR OF ELECTRON WAVE FUNCTIONS NEAR ATOMIC NUCLEUS

In the small-r region let us describe bound and continuum wave functions, apart from normalization, by the first few terms of series in r, and examine the dependence of these series on screening by a potential with a similar expansion. Consider the Schrödinger radial equation

$$R'' + 2r^{-1}R' + 2(T - V)R - l(l+1)r^{-2}R = 0 \ , \quad (2.1)$$

where V is the screened central potential and T is the kinetic energy of the electron. Taking out a function r^l with $R = r^l s$ gives

$$\tfrac{1}{2}s'' + (l+1)r^{-1}s' + (T - V)s = 0 \ . \quad (2.2)$$

For now we may normalize $s(0) \equiv 1$. For the central potential $V = -(a/r + V_0 + \tilde{V})$, with $\tilde{V}(0) = 0$, $a = Z\alpha$, the expansion of s in r begins

$$s = 1 - \frac{a}{l+1}r + \cdots \ ,$$

with the r^2 term dependent on T and V_0 but not on $\tilde{V}$. (Of course, for a bound state, T will be determined from $\tilde{V}$.) For a high-energy continuum state the result assures $Tr \ll a$. Hence until the r^2 term becomes significant s is the same as in the point-Coulomb case $V_0 = \tilde{V} = 0$.

Thus to study the behavior of s at small distances we factor out the Coulomb solution by substituting $s = s_c W$, with s_c satisfying

$$\tfrac{1}{2}s_c'' + (l+1)r^{-1}s_c' + (T_c - V_c)s_c = 0 \ , \quad (2.3)$$

where $V_c = -a/r$. Defining $\delta T \equiv T - T_c$ and $\delta V \equiv V - V_c = -(V_0 + \tilde{V})$, W satisfies

$$\frac{W''}{2} + \left(\frac{s_c'}{s_c} + \frac{l+1}{r}\right)W' + (\delta T - \delta V)W = 0 \ , \quad (2.4)$$

with $W(0) = 1$ and $W'(0) = 0$.

Consider now the bound-state case. We can calculate δT from δV with perturbation techniques. The first-order contribution is

$$-\langle i | V_0 + \tilde{V} | i \rangle = -V_0 - \langle i | \tilde{V} | i \rangle \ ,$$

with a second-order contribution

$$\sim \sum_{n \neq i} \frac{|\langle i | \tilde{V} | n \rangle|^2}{E_i - E_n} \ .$$

V_0 has no other effect. If $\tilde{V}$ is characterized by a perturbation parameter λ^2, then, neglecting $O(\lambda^4)$,

$$\delta T - \delta V \cong -\langle i | \tilde{V} | i \rangle + \tilde{V} \ . \quad (2.5)$$

Remembering that $\tilde{V}(0) = 0$ and noting that $s_c'(0)/s_c(0) = \text{const}$, we obtain W through order r^2 as

$$W = 1 + \frac{\langle i | \tilde{V} | i \rangle}{2l+3}r^2 + \cdots \ . \quad (2.6)$$

To proceed further requires discussing properties of $\tilde{V}$. (Note that to this order the result does not depend on s_c'/s_c, and so in fact does not require that the unperturbed case s_c refer to the point-Coulomb potential.)

Most analytical representations[8] of the screened potential V are analytic functions in the argument λr, giving a well-behaved power series in λr, with λ some number such as $1.13\alpha Z^{1/3}$. Since such potentials lead to satisfactory eigenfunctions and eigenvalues, we here assume that V has these properties, at least to some order in r. Other potentials are also possible, such as the $r^{1/2}$ expansion of the Thomas-Fermi case[9]; they require separate discussion but appear to lead to similar results.

We now assume

$$V = -(a/r)[1 + V_1\lambda r + V_2(\lambda r)^2 + V_3(\lambda r)^3 + \cdots] \ , \quad (2.7)$$

so that

$$V_0 = V_1\lambda a, \ \tilde{V} = V_2\lambda^2 ar + V_3\lambda^3 ar^2 + \cdots \ .$$

For example, in the simple exponential model, $V = -(a/r)e^{-\lambda r}$, $V_1 = -1$, $V_2 = \frac{1}{2}$, $V_3 = -\frac{1}{6}$, etc. Note that our assumption accords with the previous characterization of $\tilde{V}$ as being $O(\lambda^2)$. Now using[10] the expectation values of powers of r,

$$\langle i | r | i \rangle = [3n^2 - l(l+1)]/2a \ ,$$

$$\langle i | r^2 | i \rangle = n^2[5n^2 + 1 - 3l(l+1)]/2a^2 \ ,$$

we can write, neglecting $O(\lambda^4)$,

$$\begin{aligned} \delta T - \delta V \cong & -\tfrac{1}{2}[3n^2 - l(l+1)]V_2\lambda^2 \\ & - n^2[5n^2 + 1 - 3l(l+1)]V_3\lambda^3/2a \\ & + V_2\lambda^2 ar + V_3\lambda^3 ar^2 \\ \equiv & -b_0\lambda^2 + V_2\lambda^2 ar + V_3\lambda^3 ar^2 \ . \end{aligned} \quad (2.8)$$

The lowest-order result for W is then

$$W \cong 1 + \frac{b_0 \lambda^2}{2l+3} r^2$$
$$= 1 + \frac{\frac{1}{2}[3n^2 - l(l+1)] V_2 \lambda^2 r^2}{2l+3} + \cdots , \qquad (2.9)$$

which neglects relative $O(\lambda)$ in the r^2 coefficient and terms in r^3. Note that this correction is always positive. The difference in wave function for different choices of potential is also given by this formula with V_2 replaced by δV_2—the difference of the V_2 coefficient of the two potentials. If we are guided by the exponential model ($V_2 = \frac{1}{2}$), we conclude that the magnitude of deviation of wave functions from Coulomb shape at small distances is approximately

$$\frac{1}{4} \frac{3n^2 - l(l+1)}{2l+3} \alpha^2 Z^{2/3} r^2 .$$

It is possible to obtain a consistent result for W through order r^4. For this purpose one needs the first two terms in the small-r expansion of s_c'/s_c:

$$s_c = e^{-ar/n} F(l+1-n, 2l+2, 2ar/n)$$
$$\cong 1 - \frac{ar}{l+1} + \frac{2n^2 + l + 1}{(2l+2)(2l+3)} \left(\frac{ar}{n}\right)^2 ,$$
$$s_c'/s_c \cong - \frac{a}{l+1} - \frac{[n^2 - (l+1)^2] a^2 r}{(l+1)^2 (2l+3) n^2}$$
$$\equiv - \frac{a}{l+1} - da^2 r . \qquad (2.10)$$

Note also that when $n = l+1$ we have exactly $s_c'/s_c \equiv -a/n = -a/(l+1)$; i.e., there are no higher terms.

Our equation for W is now of the form

$$\frac{W''}{2} + \left(- \frac{a}{l+1} - da^2 r + \frac{l+1}{r} \right) W'$$
$$+ (-b_0 \lambda^2 + V_2 \lambda^2 a r + V_3 \lambda^3 a r^2) W = 0 , \qquad (2.11)$$

with the solution

$$W \cong 1 + \frac{b_0 \lambda^2 r^2}{2l+3} + c_3 r^3 + c_4 r^4 , \qquad (2.12)$$

where

$$b_0 = \tfrac{1}{2} [3n^2 - l(l+1)] V_2 + \frac{n^2 [5n^2 + 1 - 3l(l+1)] V_3 \lambda}{2a} ,$$

$$c_3 = \frac{[2b_0/(l+1)(2l+3) - V_2] a \lambda^2}{3(l+2)}$$
$$= \frac{[n^2 - (l+1)^2] V_2 \lambda^2 a}{(l+1)(l+2)(2l+3)}$$
$$+ \frac{n^2 [5n^2 + 1 - 3l(l+1)] V_3 \lambda^3}{3(l+1)(l+2)(2l+3)} ,$$

$$c_4 = (4l+10)^{-1} \left(3a(l+1)^{-1} c_3 \right.$$
$$\left. + \frac{2b_0 \lambda^2 a^2 [n^2 - (l+1)^2]}{n^2 (l+1)^2 (2l+3)^2} - V_3 \lambda^3 a \right) . \qquad (2.13)$$

Note that when $n = l+1$, c_3 and c_4 are of one higher order in λ. One can now see by inspection from the differential equation (2.11) that if c_3 is of higher order in λ for $n = l+1$, so will all higher-order terms in the expansion, since there are no d terms or higher. This means that for $n = l+1$ the deviations from Coulomb shape will remain small for larger r, i.e., $r \cong 1$, as long as λ is small, since the higher-order term of the expansion will remain small, $O(\lambda)$, whereas for $n \neq l+1$ all terms of the series will there be of the same magnitude. Note that the $n = l+1$ case is the nodeless case. When there are nodes and screening shifts their position even slightly, W will have singularities near the node, so the formulation is not suitable at such distances. Numerically we will see that in fact screened and Coulomb shapes remain close even beyond the first node.

How is this analysis modified for continuum states? We have already noted the requirement $Tr \ll a$ for the expansion

$$s = 1 - \frac{a}{l+1} r + \cdots .$$

For T and r which do not satisfy the requirement—for example, $Tr = O(1)$—one is already in the oscillatory region of the wave function. The same requirement enters Eq. (2.4) for W in the factor s_c'/s_c. One understands the necessity for this on realizing that once again screening is shifting the position of nodes and at such points W must diverge. For high energies this requirement, $Tr \ll a$, is in fact unnecessarily restrictive in a discussion of screening effects, but the present techniques cannot be used; we will show some numerical results.

For the low-energy case $T \leq O(a^2)$ we may use our previous analysis. The only difference is how we specify δT, the change in kinetic energy of Coulomb and screened calculation. Since T is no longer calculated from V for continuum states, one would expect $\delta T = 0$. But in fact this is generally not the correct physical choice. For example, in the atomic photoeffect with a given incident photon energy, if the bound-state energy is shifted δT_B because of screening, the ejected continuum electron will also have an energy shift $\delta T = \delta T_B$ and a shape considerably closer to the Coulomb shape at small distances than for $\delta T = 0$. A shape even closer to point-Coulomb results from the choice $\delta T = -V_0$, for the r^2 term in W then vanishes. Noting that V_0 has the opposite sign for a positron (changing the sign of V), we realize that this is the proper choice to make for pair production: For

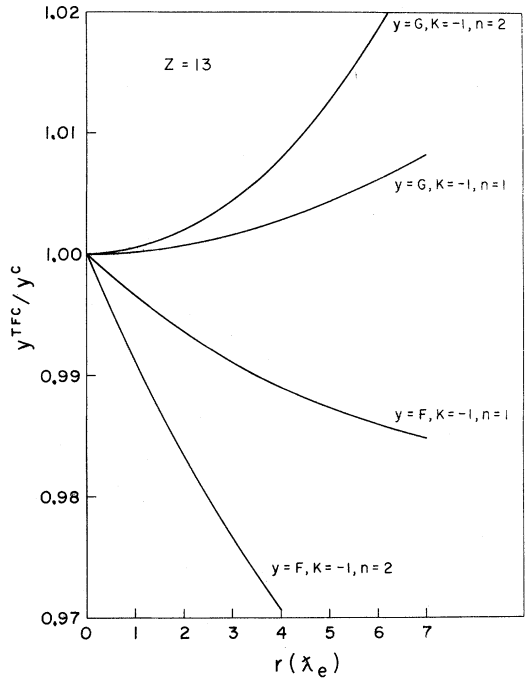

FIG. 1. Screening effects on the shape of Dirac radial bound-state wave functions G and F near the atomic nucleus for $Z=13$. ($\lambda\!\!\!^{-}_e$ in the figure is the Compton wavelength.)

a given incident photon energy, point-Coulomb production of (E_+, E_-) should be compared with a screened production of $(E_+ + V_0,\ E_- - V_0)$.

We may summarize the lowest-order results for W in these three cases:

(i) $\delta T = 0$,

$$W \cong 1 - \frac{V_0 r^2}{2l+3} = 1 - \frac{V_1 a\lambda r^2}{2l+3}\ ;$$

(ii) $\delta T = \delta T_B$,

$$W \cong 1 + \frac{\langle i|\tilde{V}|i\rangle r^2}{2l+3}$$

$$\cong 1 + \frac{[3n^2 - L(L+1)]V_2\lambda^2 r^2}{2(2l+3)}\ ,$$

with l and L continuum and bound orbital quantum numbers;

(iii) $\delta T = -V_0$,

$$W \cong 1 - \frac{V_2 a\lambda^2 r^3}{3(l+2)}\ .$$

The relative orders of the deviations are as a, λ, and ar, respectively.

Our conclusion thus far is that deviations from Coulomb shapes remain rather small out to several Compton wavelengths because they are characterized not by ar or $(ar)^2$ but by something like $\alpha^2 Z^{2/3} r^2$. We have carried out a similar analysis for the coupled radial wave functions of the Dirac equation and have verified that relativistic effects do not change the conclusion that deviations from Coulomb shape are small at these distances. The algebra is considerably more complicated and we shall not reproduce it here. Some features do differ from the nonrelativistic case.[11] Most of these differences can already be seen in the Klein-Gordon case with its extra V^2 term. As a result there are extra screening-dependent terms of relative order a/r—at small r there are now linear as well as quadratic screening terms in r, but by Compton-wavelength distances the quadratic terms will dominate, so our earlier estimates still apply. In addition, in the Dirac case the linear term of the small-component wave function has a significant energy dependence, resulting in a greater dependence on screening.

We now illustrate these ideas by showing in Figs. 1–4 and Tables I–III the point-Coulomb and screened wave functions (omitting the normalization) obtained in numerical calculations with the Dirac equation. The cases were chosen to give some coverage of large and small components, bound and continuum states (with the different energy-shift choices), low and high Z, and dependence on energy and κ. For high-Z elements, to show that agreement persists beyond the first node, we have presented the wave functions in tables instead of figures. The screening effect on the low-κ par-

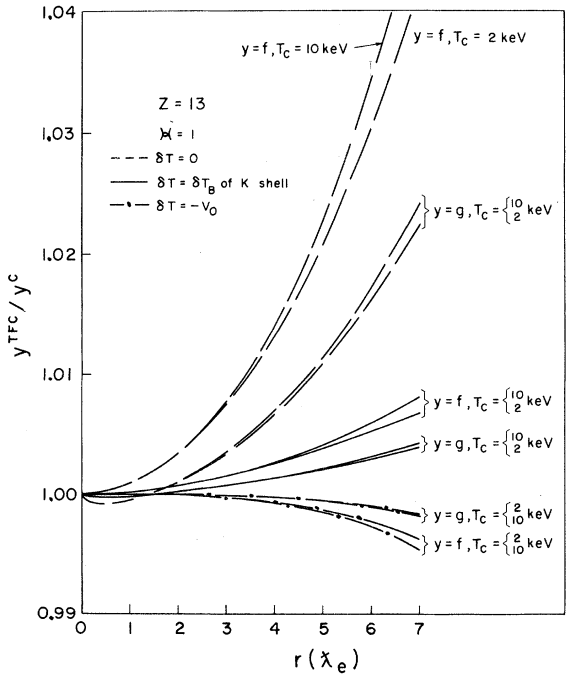

FIG. 2. Screening effects on the shape of Dirac radial continuum-state wave functions g and f near the atomic nucleus for $Z=13$, $T_c=2$ and 10 keV, and $\kappa=1$.

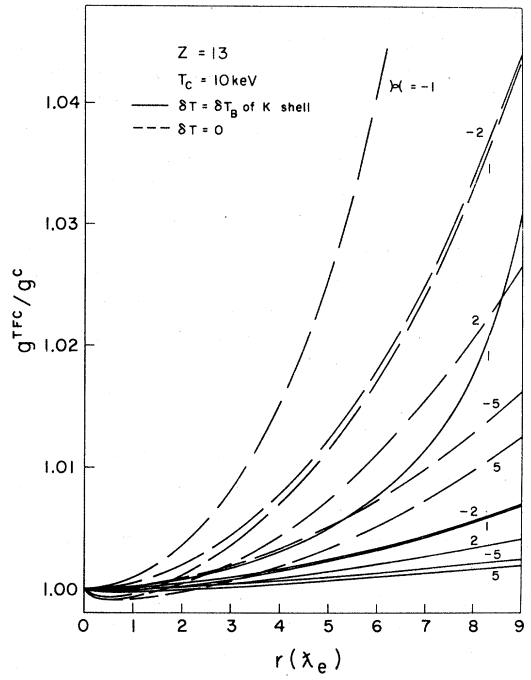

FIG. 3. Same as Fig. 2 except for the large-component continuum-state wave function g and $Z=13$, $T_c=10$ keV, and $\kappa=-1, +1, -2, +2, -5, +5$.

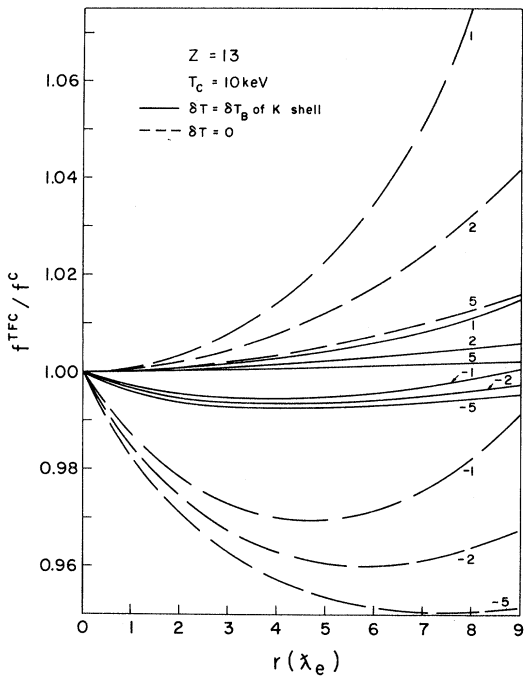

FIG. 4. Same as Fig. 3 except for the small-component continuum-state wave function f.

tial-wave continuum wave function with energy shift is similar to that of the large-component bound-state wave function at small distances. For continuum wave functions the screening effect is smaller for the case with energy shift than without energy shift as expected. At $r=O(\frac{1}{2})$ the screening effect to the shape of the continuum-state wave function is very small both for the cases with and without energy shift. This is the result needed for the low-energy screening theory of atomic pair production.[5] We see also that, for large-compo-

TABLE I. Shape of Dirac radial bound-state wave functions G and F (omitting the normalization) near the atomic nucleus for $Z=92$. Symbols C and TFC refer to point-Coulomb and modified Thomas-Fermi potentials, respectively. ($λ\!\!\!^-_e$ is the Compton wavelength.)

r	$Z=92$, K shell				$Z=92$, L_I shell			
($λ\!\!\!^-_e$)	G_C	G_{TFC}	F_C	F_{TFC}	G_C	G_{TFC}	F_C	F_{TFC}
0.2	0.874 36	0.874 60	−0.337 13	−0.337 07	0.847 72	0.848 61	−0.343 39	−0.343 19
0.4	0.764 50	0.764 96	−0.294 77	−0.294 69	0.711 76	0.713 48	−0.305 20	−0.304 91
0.6	0.668 44	0.669 10	−0.257 73	−0.257 64	0.590 60	0.593 08	−0.270 66	−0.270 34
0.8	0.584 46	0.585 27	−0.225 35	−0.225 27	0.482 83	0.485 98	−0.239 44	−0.239 16
1.0	0.511 02	0.511 96	−0.197 04	−0.196 97	0.387 17	0.390 90	−0.211 25	−0.211 06
1.4	0.390 67	0.391 79	−0.150 63	−0.150 61	0.227 67	0.232 23	−0.162 91	−0.162 95
1.8	0.298 67	0.299 88	−0.115 16	−0.115 18	0.103 96	0.108 95	−0.123 73	−0.124 05
2.2	0.228 33	0.229 56	−0.088 04	−0.088 10	0.009 33	0.014 35	−0.092 13	−0.092 73
2.6	0.174 56	0.175 75	−0.067 31	−0.067 40	−0.061 81	−0.057 09	−0.066 78	−0.067 62
3.0	0.133 45	0.134 58	−0.051 45	−0.051 58	−0.114 04	−0.109 90	−0.046 56	−0.047 60
3.4	0.102 02	0.103 06	−0.039 34	−0.039 47	−0.151 16	−0.147 80	−0.030 57	−0.031 75
3.8	0.078 00	0.078 93	−0.030 07	−0.030 21	−0.176 28	−0.173 85	−0.018 03	−0.019 30
4.2	0.059 63	0.060 46	−0.022 99	−0.023 13	−0.191 96	−0.190 55	−0.008 30	−0.009 61
4.6	0.045 59	0.046 31	−0.017 58	−0.017 71	−0.200 26	−0.199 93	−0.000 85	−0.002 16
5.0	0.034 85	0.035 47	−0.013 44	−0.013 57	−0.202 89	−0.203 63	0.004 75	0.003 48
5.4	0.026 64	0.027 17	−0.010 27	−0.010 39	−0.201 22	−0.203 00	0.008 86	0.007 67
5.8	0.020 37	0.020 80	−0.007 85	−0.007 97	−0.196 35	−0.199 12	0.011 79	0.010 69
6.2	0.015 57	0.015 92	−0.006 00	−0.006 11	−0.189 17	−0.192 86	0.013 77	0.012 78
6.6	0.011 90	0.012 18	−0.004 59	−0.004 69	−0.180 39	−0.184 90	0.015 01	0.014 14
7.0	0.009 10	0.009 30	−0.003 51	−0.003 60	−0.170 57	−0.175 81	0.015 67	0.014 92

TABLE II. Shape of Dirac radial continuum-state wave function g near the atomic nucleus for $Z=92$, $T_c=60$ and 100 keV, and $\kappa=1$. Symbols $g_{TFC}(1)$, $g_{TFC}(2)$, and $g_{TFC}(3)$ refer to $\delta T=0$, $\delta T=\delta T_B$ of K shell and $\delta T=-V_0$, respectively.

r	$Z=92$, $T_c=60$ keV, $\kappa=1$				$Z=92$, $T_c=100$ keV, $\kappa=1$			
(λ_e)	g_C	$g_{TFC}(1)$	$g_{TFC}(2)$	$g_{TFC}(3)$	g_C	$g_{TFC}(1)$	$g_{TFC}(2)$	$g_{TFC}(3)$
0.2	1.287 5	1.286 3	1.287 4	1.287 5	1.290 5	1.289 4	1.290 4	1.290 5
0.4	1.510 2	1.511 4	1.510 3	1.510 2	1.506 4	1.508 0	1.506 6	1.506 5
0.6	1.673 2	1.680 4	1.673 7	1.673 3	1.653 4	1.661 3	1.654 0	1.653 5
0.8	1.781 8	1.798 2	1.782 8	1.781 8	1.737 5	1.754 9	1.738 6	1.737 5
1.0	1.841 2	1.869 5	1.842 8	1.841 0	1.765 0	1.794 6	1.766 6	1.764 8
1.4	1.833 0	1.891 9	1.835 8	1.832 0	1.676 7	1.736 2	1.679 4	1.675 6
1.8	1.689 2	1.783 9	1.692 8	1.686 8	1.441 9	1.534 1	1.445 4	1.439 5
2.2	1.448 2	1.579 6	1.452 2	1.443 8	1.112 9	1.235 0	1.116 5	1.108 7
2.6	1.145 2	1.309 9	1.149 0	1.138 5	0.738 00	0.882 32	0.741 15	0.732 02
3.0	0.811 73	1.002 4	0.814 64	0.802 60	0.359 61	0.514 46	0.361 77	0.352 06
3.4	0.474 73	0.681 05	0.476 33	0.463 42	0.012 33	0.163 78	0.013 25	0.003 90
3.8	0.156 41	0.366 04	0.156 50	0.143 58	−0.277 87	−0.144 29	−0.278 14	−0.286 15
4.2	−0.125 93	0.073 74	−0.127 28	−0.139 29	−0.494 06	−0.391 66	−0.495 14	−0.500 92
4.6	−0.359 89	−0.183 30	−0.362 31	−0.372 52	−0.628 07	−0.567 47	−0.629 31	−0.632 19
5.0	−0.537 72	−0.396 18	−0.540 59	−0.548 19	−0.679 76	−0.667 79	−0.680 41	−0.679 96
5.4	−0.656 02	−0.559 42	−0.658 51	−0.662 86	−0.655 87	−0.694 76	−0.655 17	−0.651 32
5.8	−0.715 18	−0.670 72	−0.716 39	−0.717 07	−0.568 54	−0.655 70	−0.565 87	−0.558 90
6.2	−0.718 89	−0.730 53	−0.717 94	−0.714 76	−0.433 63	−0.561 91	−0.428 65	−0.419 16
6.6	−0.673 48	−0.741 71	−0.669 61	−0.662 64	−0.269 04	−0.427 39	−0.261 81	−0.250 66
7.0	−0.587 23	−0.709 06	−0.579 93	−0.569 54	−0.093 07	−0.267 58	−0.084 03	−0.072 27

nent continuum wave functions, the higher the κ partial waves, the smaller the screening effect on the wave function shape. For small-component continuum wave functions for the positive-κ partial waves we have the same conclusion as for the large-component continuum wave functions, while for the negative-κ partial waves we have the inverse conclusion.

In this paper we are concerned with the shape of electron wave functions. A second related question concerns the normalization of electron wave functions. Although we do not here wish to discuss the theory of the normalization constants, for completeness we give some numerical results. Consider first the continuum case. For high energies we have noted that the deviation from Coulomb normalization is small. For very low energies we had noted[3] that continuum Coulomb wave functions vary as $(pE)^{-1/2}$. Now, in photoeffect and other similar processes the matrix element is multiplied by

TABLE III. Same as Table II except for the wave function f of $Z=92$ and $T_c=60$ and 100 keV.

r	$Z=92$, $T_c=60$ keV, $\kappa=1$				$Z=92$, $T_c=100$ keV, $\kappa=1$			
(λ_e)	f_C	$f_{TFC}(1)$	$f_{TFC}(2)$	$f_{TFC}(3)$	f_C	$f_{TFC}(1)$	$f_{TFC}(2)$	$f_{TFC}(3)$
0.2	2.279 8	2.291 0	2.280 4	2.279 7	2.250 6	2.261 8	2.251 13	2.250 6
0.4	1.984 8	2.007 5	1.986 0	1.984 6	1.925 6	1.948 2	1.926 9	1.925 4
0.6	1.708 8	1.742 9	1.710 6	1.708 5	1.620 3	1.654 0	1.622 1	1.619 9
0.8	1.452 2	1.497 1	1.454 4	1.451 6	1.336 2	1.380 0	1.338 3	1.335 5
1.0	1.215 0	1.269 7	1.217 4	1.214 0	1.074 3	1.127 0	1.076 6	1.073 3
1.4	0.798 29	0.868 78	0.800 78	0.796 32	0.620 18	0.685 35	0.622 45	0.618 33
1.8	0.456 75	0.536 86	0.458 84	0.453 78	0.260 36	0.330 12	0.262 13	0.257 73
2.2	0.186 65	0.269 54	0.188 01	0.182 80	−0.007 27	0.058 85	−0.006 29	−0.010 42
2.6	−0.017 19	0.061 72	−0.016 72	−0.021 63	−0.188 88	−0.133 82	−0.188 74	−0.192 11
3.0	−0.161 14	−0.092 28	−0.161 53	−0.165 71	−0.293 89	−0.255 69	−0.294 43	−0.296 66
3.4	−0.252 40	−0.198 56	−0.253 45	−0.256 59	−0.334 07	−0.316 37	−0.334 99	−0.335 83
3.8	−0.298 74	−0.263 46	−0.300 14	−0.301 99	−0.322 68	−0.326 70	−0.323 57	−0.322 96
4.2	−0.308 16	−0.293 43	−0.309 53	−0.309 96	−0.273 49	−0.298 09	−0.273 97	−0.272 00
4.6	−0.288 62	−0.294 84	−0.289 57	−0.288 58	−0.200 02	−0.241 92	−0.199 79	−0.196 71
5.0	−0.247 81	−0.273 87	−0.248 00	−0.245 69	−0.114 77	−0.169 05	−0.113 66	−0.109 85
5.4	−0.192 90	−0.236 36	−0.192 07	−0.188 64	−0.028 65	−0.089 30	−0.026 69	−0.022 56
5.8	−0.130 38	−0.187 70	−0.128 39	−0.124 12	0.049 45	−0.011 11	0.052 09	0.056 05
6.2	−0.065 89	−0.132 77	−0.062 77	−0.057 99	0.112 96	0.058 71	0.115 92	0.119 29
6.6	−0.004 20	−0.075 84	−0.000 11	0.004 82	0.157 67	0.115 13	0.160 49	0.162 89
7.0	0.050 95	−0.020 55	0.055 71	0.060 41	0.181 66	0.154 99	0.183 86	0.185 03

TABLE IV. Screening effects on the continuum-state normalizations. Symbols c, s, WO, WK, and WL_{I} refer to point-Coulomb potential, modified Thomas-Fermi potential, results without energy shift ($\delta T=0$), results with $\delta T=\delta T_B$ of K shell, and results with $\delta T=\delta T_B$ of L_{I} shell, respectively.

$\tilde{N}_s/\tilde{N}_c$ ($Z=13$)	WO	WK	WL_{I}	WO	WK	WL_{I}	WO	WK	WL_{I}	WO	WK	WL_{I}
κ \ T_c (keV)		2			5			10			100	
−1	0.998	0.999	0.998	0.995	0.999	0.998	0.994	0.999	0.997	0.997	0.999	0.999
+1	0.872	0.981	0.933	0.922	0.987	0.958	0.951	0.991	0.973	0.993	0.999	0.996
−2	0.871	0.981	0.932	0.922	0.987	0.958	0.950	0.991	0.973	0.992	0.998	0.995
+2	0.728	0.994	0.873	0.848	0.988	0.924	0.909	0.989	0.953	0.987	0.997	0.993
−5	0.554	1.13	0.842	0.741	1.03	0.890	0.842	1.001	0.927	0.976	0.996	0.987
+5	0.503	1.25	0.857	0.704	1.06	0.887	0.816	1.013	0.920	0.971	0.996	0.985
−10	0.391	2.07	1.04	0.607	1.28	0.923	0.741	1.10	0.920	0.953	0.997	0.977
+10	0.375	2.39	1.11	0.591	1.35	0.942	0.728	1.12	0.925	0.950	0.998	0.976
$\tilde{N}_s/\tilde{N}_c$ ($Z=92$)	WO	WK	WL_{I}	WO	WK	WL_{I}	WO	WK	WL_{I}	WO	WK	WL_{I}
κ \ T_c (keV)		10			50			100			400	
−1	0.985	1.000	0.997	0.986	0.999	0.997	0.987	0.999	0.997	0.990	0.999	0.998
+1	0.939	0.997	0.988	0.952	0.997	0.990	0.961	0.998	0.992	0.982	0.999	0.996
−2	0.909	0.997	0.983	0.927	0.998	0.986	0.940	0.998	0.989	0.968	0.999	0.994
+2	0.741	1.005	0.963	0.847	1.000	0.975	0.893	0.999	0.981	0.956	0.998	0.991
−5	0.345	1.20	1.03	0.662	1.05	0.978	0.771	1.02	0.976	0.904	1.001	0.985
+5	0.241	1.40	1.14	0.601	1.08	0.993	0.732	1.03	0.980	0.894	1.002	0.984
−10	0.0870	4.06	2.61	0.427	1.39	1.16	0.592	1.15	1.04	0.820	1.02	0.985
+10	0.0732	5.53	3.37	0.401	1.48	1.22	0.571	1.19	1.06	0.812	1.02	0.986

$(pE)^{1/2}$ for each final electron. It is thus appropriate to look at $\tilde{N}\equiv(pE)^{1/2}N$, where N is the continuum-state normalization, which we find is nearly independent of screening. We demonstrate this in numerical calculation, and, as in the case of shape, best agreement is obtained if we compare the continuum Coulomb wave function with the screened wave function of shifted energy. We show these results in Table IV, where we have used K and L_I shifts in view of our prospective application to the photoeffect. For low-κ partial waves except at very low energies $\tilde{N}_s\equiv(p_sE_s)^{1/2}N_s$ is equal to $\tilde{N}_c\equiv(p_cE_c)^{1/2}N_c$ for the case with energy shift. At high energies even for high-κ partial waves $\tilde{N}_s$ is equal to $\tilde{N}_c$ for the cases with or without energy shift. The worst cases are for high κ at low energies, which are not of concern in most processes. For example, for the atomic photoeffect, the process that we will consider in Sec. III in detail, the low-κ partial waves dominate the cross section for low photon energies. Therefore we may conclude that for the atomic photoeffect $\tilde{N}_s$ is equal to $\tilde{N}_c$.

For bound states, we present values of the square of the ratio of screened (s) to point-Coulomb (c) bound-state normalization[12] for states K, L_{I}, L_{II}, and L_{III} in Table V in five different potentials, i.e., the ionic HFS$\frac{2}{3}$ (ionic),[13] the Kohn-Sham (HFS$\frac{2}{3}$),[14] the Hartree-Fock-Slater (HFS),[7] the modified Thomas-Fermi (TFC),[15] and the Thomas-Fermi (TF)[16] potential models. This shows that for low Z the choice of the model is quite important. For high Z the difference is less than 1% for the K shell, less than 3.5% for the L_{I} shell, and less than 8% for L_{II} and L_{III} shells. Finally, we tabulate values of the square of the ratio of the HFS to point-Coulomb bound-state normalizations for the K, L_{I}, L_{II}, and L_{III} shells in Table VI for elements $Z=13$–92. We can see that the screening effect is more important for low Z and much more important for higher shells—1–5% for the K shell over the same range of Z, 10–70% for the L shell.

TABLE V. Square of the ratio Ξ of screened to point-Coulomb bound-state normalizations for states K, L_{I}, L_{II}, and L_{III}, where $\Xi\equiv\lim_{r\to0}G^s(r)/G^c(r)=\lim_{r\to0}F^s(r)/F^c(r)$. (Here G and F are the bound-state wave functions without omitting normalization.)

Z	Potentials	K	L_{I}	L_{II}	L_{III}
13	Ionic	0.9659	0.5257	0.3319	0.3306
	HFS$\frac{2}{3}$	0.9286	0.4996	0.3025	0.3012
	HFS	0.9479	0.5260	0.3360	0.3346
	TFC	0.9065	0.4546	0.2355	0.2346
	TF	0.8823	0.4633	0.2461	0.2452
92	Ionic	0.9905	0.8895	0.8370	0.7999
	HFS$\frac{2}{3}$	0.9819	0.8829	0.8251	0.7899
	HFS	0.9868	0.8905	0.8378	0.8011
	TFC	0.9915	0.9127	0.8860	0.8508
	TF	0.9897	0.8866	0.8344	0.8019

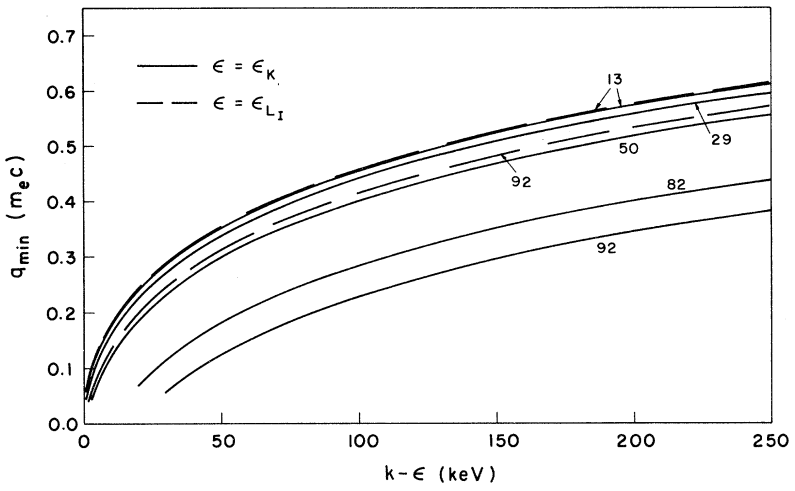

FIG. 5. Values of the minimum momentum transfer $q_{\min}$ above the K shell and above the L_{I} shell. The eigenvalues ϵ_K are given in Table VII; $\epsilon_{L_{\mathrm{I}}}$ for $Z=13$ and 92 are 0.000 199 9 and 0.043 23$m_e c^2$, respectively.

III. NORMALIZATION SCREENING THEORY IN ATOMIC PHOTOEFFECT

Following the formalism of the earlier photoeffect work,[3] we write the differential cross section for the atomic field photoeffect as

$$d\sigma/d\Omega = (2\pi)^{-2} pE\,|M_{fi}|^2 , \tag{3.1}$$

subject to energy conservation, with

$$M_{fi} = (2\pi\alpha/k)^{1/2} \int d^3 r \psi_f^\dagger \vec{\alpha}\cdot\vec{\epsilon}\,\psi_i e^{i\vec{k}\cdot\vec{r}} . \tag{3.2}$$

Here ψ_i is the initial bound-state wave function square normalized to unity with binding energy ϵ, and ψ_f is the final continuum-state wave function asymptotically normalized to a unit-amplitude modified plane wave of four-momentum $(E,\vec{p})$ plus an incoming spherical wave. The incident radiation is specified by four-momentum $(k,\vec{k})$ and four-polarization $(0,\vec{\epsilon})$.

The normalization screening theory[2,3] works for energies well above threshold because the minimum possible momentum transfer to the nucleus $q_{\min}$ is of order 1, so that the most important regions of configuration space $r_{\max}$ for the photoeffect matrix element are of the order of the electron Compton wavelength. Contributions from larger distances are cut off fairly sharply, perhaps reaching the 1% level by $3-5r_{\max}$, where $r_{\max}\equiv q_{\min}^{-1}$. We calculate $q_{\min}=p-k$ using the energy conservation relation $k+1-\epsilon=(1+p^2)^{1/2}$. In Fig. 5 we give values of $q_{\min}$ for various choices of k and ϵ. We note in passing the interesting fact that, given an electron bound by ϵ, there exists one photon energy k ($\cong\epsilon+\frac{1}{2}\epsilon^2$) for which the electron can be ejected without any momentum transfer.

By using the properties of electron wave functions at small distances discussed in Sec. II we wish here to estimate roughly to how low an energy the normalization screening theory should be believed. The change in cross section is then determined from

$$\sigma \sim \left(\int_0^{r_{\max}} dr\, r^{L+2} W_{\text{bound}}\, W_{\text{continuum}}\right)^2$$

$$\sim r_{\max}^{2L+6}(1+\Delta) , \tag{3.3}$$

with

$$\Delta \cong 4(L+3)(L+5)^{-1}(2L+3)^{-1}$$

$$\times [3n^2 - L(L+1)]\left(\tfrac{1}{2}V_2\right)\lambda^2 r_{\max}^2$$

characterizing the magnitude of the deviation from a simple normalization description of screening. We have assumed that continuum effects are approximately the same as bound-state effects. We find that the choice of screened-potential model does not change the estimate of Eq. (3.3) greatly. As an illustration we chose the modified Thomas-Fermi potential model (TFC).[15] The nice feature of this model is that the potential is written analytically, namely,

$$V(r) = (-a/r)(0.7111e^{-0.175a_0 r} + 0.2889e^{-1.6625a_0 r})^2 \tag{3.4}$$

TABLE VI. Values of $(\Xi^2)_{\mathrm{HFS}}$ for $Z=13-92$.

Z	K	L_{I}	L_{II}	L_{III}
13	0.9479	0.5260	0.3360	0.3346
20	0.9615	0.6509	0.4928	0.4899
26	0.9686	0.7133	0.5790	0.5745
29	0.9713	0.7354	0.6112	0.6058
42	0.9784	0.7968	0.7016	0.6915
47	0.9801	0.8128	0.7254	0.7134
50	0.9810	0.8211	0.7377	0.7244
60	0.9832	0.8443	0.7717	0.7540
74	0.9853	0.8689	0.8072	0.7824
79	0.9859	0.8757	0.8170	0.7892
82	0.9861	0.8794	0.8223	0.7927
92	0.9868	0.8905	0.8378	0.8011

TABLE VII. Estimations of the correction Δ of the normalization screening theory for the K-shell atomic-field photoeffect cross section.

Z	13	29	50	82	92
$\epsilon_K/(m_e c^2)$	0.002 801 5	0.017 122	0.056 933	0.174 69	0.230 53
$k-\epsilon_K$ (keV)					
4	0.03	...	...	...	...
5	0.024	0.06	...	...	...
7.5	0.016	0.04	...	...	...
10	0.010	0.03	0.06	...	...
20	0.006	0.014	0.03	...	...
30	0.004	0.010	0.02	...	...
40	0.004	0.008	0.014	...	...
50	0.004	0.006	0.012	...	...
60	0.002	0.006	0.010	0.03	...
80	0.002	0.004	0.008	0.02	0.03
100	0.002	0.004	0.006	0.016	0.02
150	0.002	0.002	0.004	0.010	0.014
200	0.002	0.002	0.004	0.008	0.010
250	0.001	0.002	0.004	0.006	0.008

with

$$a_0 = 2(\tfrac{3}{4}\pi)^{-2/3}\alpha Z^{1/3} .$$

In order to calculate Δ given by Eq. (3.3) we need the binding energy ϵ, which was calculated numerically by solving the bound-state Dirac wave equations. The binding energies are given in Table VII. We may now tabulate the values of the correction Δ to the normalization screening theory. For the K shell the values of Δ are given in Table VII. We also find that the normalization screening theory can be good to 1% for photon energies more than 40 keV above the L_I-shell threshold in Al, 100 keV in Cu, 250 keV in Sn, 500 keV in Pb, and 600 keV in U; and to 2% for photon energies more than 20 keV above the L_I-shell threshold in Al, 40 keV in Cu, 80 keV in Sn, 150 keV in Pb, and 150 keV in U. However, since the K shell contributes more than 80% of the total cross section for the cases in which the K-shell cross section dominates the total cross section, we may conclude that this theory can be good to 1% for photon energies more than 10 keV above the K-shell threshold in Al, 30 keV in Cu, 60 keV in Sn, 150 keV in Pb, and 200 keV in U. It is apparent that this theory will achieve higher accuracy only above the K threshold.

For the above estimates we have also used Dirac wave functions; the results agree quite well with the nonrelativistic Schrödinger treatment.

Let us now compare our estimates with actual numerical calculations. By using the recent results of Scofield[6] for the HFS potential and the point-Coulomb results of Hultberg, Nagel, and Olsson (HNO)[17] we show the error of the normalization screening theory (NT)

$$\mathrm{NE} \equiv [\sigma(\mathrm{NT}) - \sigma(\mathrm{Scofield})]/\sigma(\mathrm{Scofield})$$

in Table VIII for the K shell. Here we find that the normalization screening theory can be good to 1% for the K shell for photon energies more than 8 keV above the K-shell threshold in Al, 25 keV in Cu, 30 keV in Sn, and 80 keV in U. These results agree well in order of magnitude with our estimates. For the higher-Z cases the shape deviation appears in fact quite close to $\frac{1}{2}\Delta$. For L_I shell our results agree also quite well with the results which were calculated with the computer code of Rakavy and Ron.[18]

TABLE VIII. Error of the normalization screening theory (NE) based on the K-shell atomic-field photoeffect cross sections of Scofield (see Ref. 6) with HFS potential and of HNO (see Ref. 17) with point-Coulomb potential.

Z	13	29	50	82	92
k (keV)					
5	0.030	...	...	...	...
6	0.023	...	...	...	...
8	0.015	...	...	...	...
10	0.010	...	...	...	...
15	0.004	...	...	...	...
20	0.001	...	...	...	...
30	−0.002	0.013	...	...	...
40	−0.003	0.008	...	...	...
50	−0.005	0.003	0.11	...	...
60	−0.004	0.002	0.01	...	...
80	−0.005	0.002	0.01	...	...
100	−0.004	0.002	0.01	...	...
150	−0.004	−0.001	0.005	...	...
200	−0.003	−0.001	0.004	0.008	0.007
300	−0.003	−0.001	0.002	0.006	0.007
400	−0.002	−0.002	0.001	0.006	0.006

These ideas can also be used to predict model- and energy-independent ratios of cross sections for states having the same angular momentum. This follows[11] because in a given atom the bound-state wave functions of same angular momentum but different n are proportional in the important region $r = O(1)$, and the proportionality is independent of Z. Angular distributions and polarization correlations from such states are the same.

ACKNOWLEDGMENT

We wish to thank Dr. A. Ron for helpful discussions.

*Supported in part by the Lawrence Radiation Laboratory of the University of California under Subcontracts Nos. 6985207 and 4738209 and in part by U.S. Atomic Energy Commission under Contract No. AT-(30-1)-3829.

[1](a)This has long been exploited in many investigations of nuclear-physics questions, such as hyperfine structure,

β decay, etc. See, for example, G. Breit, Phys. Rev. 38, 463 (1931); J. E. Rosenthal and G. Breit, *ibid.* 41, 459 (1932); E. Fermi and E. Segrè, Z. Physik 82, 729 (1933); M. E. Rose, Phys. Rev. 49, 729 (1936). (b) H. Brysk and M. E. Rose, Rev. Mod. Phys. 30, 1169 (1958).

[2]R. H. Pratt, Phys. Rev. 119, 1619 (1960).

[3]R. D. Schmickley and R. H. Pratt, Phys. Rev. 164, 104 (1967).

[4]I. M. Band, L. A. Sliv, and M. B. Trzhaskovskaya, Institute of Technical Physics Report No. 262, 1970 (unpublished) (order No. 1314, 21/IV).

[5]H. K. Tseng and R. H. Pratt, Phys. Rev. A 4, 1835 (1971).

[6]A. Ron (private communication); J. Scofield (private communication). We wish to thank Dr. Ron and Dr. Scofield for kindly sending us their recent atomic photoeffect results.

[7]D. Liberman, J. T. Waber, and D. T. Cromer, Phys. Rev. 137, A27 (1965); J. Scofield (private communication). We wish to thank Dr. Scofield for kindly sending us the bound-state normalization constants.

[8]See, for example, W. J. Byatt, Phys. Rev. 104, 1298 (1956).

[9]E. B. Baker, Phys. Rev. 36, 630 (1930).

[10]See, for example, L. D. Landau and E. M. Lifshitz, *Quantum Mechanics*, translated from the Russian by J. B. Sykes and J. S. Bell (Addison-Wesley, Reading, Mass., 1958), p. 125.

[11]R. H. Pratt, Phys. Rev. 119, 1619 (1960); 120, 1717 (1960). For processes which are very sensitive to the series expansion of $V(r)$ further difficulties arise. For the self-consistent potential without the exchange term, for instance, the relativistic series expansions of $V(r)$ are different from the nonrelativistic one.

Relativistic expansion:

$$V(r) = -\left(\frac{a}{r} + V_0 + \frac{\alpha N_K^2}{\gamma(2\gamma+1)}\, r^{2\gamma} + \cdots\right)$$

[see, for example, R. C. Barrett, S. J. Brodsky, G. W. Erickson, and M. M. Goldhaber, Phys. Rev. 166, 1589 (1968)], where N_K is the normalization of the K-shell electrons, $N_K^2 = (2a)^{2\gamma+1}/\Gamma(2\gamma+1)$, $\gamma = (1-a^2)^{1/2}$, and $a = Za$.

Nonrelativistic expansion:

$$V(r) = -(a/r + V_0' + \tfrac{1}{3}\alpha N_K'^2\, r^2 + \cdots), \quad N_K'^2 = 4a^3.$$

In the nonrelativistic case Slater exchanges give constant and linear terms, while in the relativistic case these are multiplied by $r^{2\gamma/3}$. In practice it has proved satisfactory to begin numerical calculations with ordinary power-series fits of the potential at Compton-wavelength distances.

[12]Nonrelativistically the normalizations of bound states are related to the binding energies of the bound states, for instance, the well-known Fermi-Segrè formula. See, for example, L. L. Foldy, Phys. Rev. 111, 1093 (1958); M. J. Seaton, Monthly Notices Roy. Astron. Soc. 118, 504 (1958); U. Fano, Phys. Rev. A 2, 353 (1970).

[13]D. A. Liberman, Phys. Rev. B 2, 244 (1970); D. A. Liberman, D. T. Cromer, and J. T. Waber, Computer Phys. Commun. 2, 107 (1971). We wish to thank Dr. Liberman for kindly sending us the relativistic self-consistent-field computer code for calculating the ionic HFS$\frac{1}{3}$ potential. Note that the "ionic" code is for calculation of the neutral atom, but recognizes that each electron sees only an ion.

[14]W. Kohn and L. S. Sham, Phys. Rev. 140, A1133 (1965).

[15]P. Csavinszky, Phys. Rev. 166, 53 (1968).

[16]L. H. Thomas, Proc. Cambridge Phil. Soc. 23, 542 (1927); E. Fermi, Z. Physik 48, 73 (1928).

[17]S. Hultberg, B. Nagel, and P. Olsson, Arkiv Fysik 38, 1 (1968).

[18]G. Rakavy and A. Ron, Phys. Rev. 159, 50 (1967).